minerals

MDPI

Article

Heavy Metal Regularity of Carboniferous Weathered Black Shale in Qiziqiao Area, Central Hunan

Wanghu He [1], Deqiu Dai [1,2,*], Bozhi Ren [1,2], Zhanyu Tang [1] and Yu Qiu [1]

[1] School of Earth Sciences and Spatial Information Engineering, Hunan University of Science and Technology, Xiangtan 411201, China; 21010103003@mail.hnust.edu.cn (W.H.)
[2] Hunan Provincial Key Laboratory of Shale Gas Resource Utilization, Hunan University of Science and Technology, Xiangtan 411201, China
* Correspondence: 1020099@hnust.edu.cn

Abstract: The Hunan region is a high geological background area of black rock series rich in various metallic elements; accordingly, local heavy metal pollution is severe. Previous studies on black shale have primarily focused on the lower Cambrian strata, while research on Carboniferous black shale remains scarce. To better explore the activity law of heavy metals during Carboniferous black shale weathering, this study analyzed the elemental components of samples through field observations of outcrops in the Qiziqiao area of central Hunan province, China using inductively coupled plasma mass spectrometry and X-ray fluorescence spectrometry. The results showed that the heavy metal content of black shale under different degrees of weathering varied greatly, with different heavy metals maintaining distinct migration and enrichment rules throughout this process. The heavy metal content in Carboniferous black shale and soils of central Hunan was generally less than that of the regional lower Cambrian black shale and soil; however, the Cd content in the black shale soil was slightly higher than background values, while the Sr content was substantially higher than background values. Heavy metals V, Cr, Co, Ni, Cu, and Pb were not generally leached or released during weathering, and may undergo relative enrichment or secondary enrichment. Comparatively, Zn, Cd, and Ba can be more readily leached and released, and may undergo secondary enrichment. The lithophilic element Sr tended to leach out overall and expressed strong activity, whereas the chemical activities of the high-field-strength elements, Zr and Hf, were relatively stable. During soil formation, all heavy metal elements save Sr were significantly enriched. The enrichment factor analysis of different degrees of weathered black shale reveals that the heavy metals Ba, Hf, and Sr in black shale soil originate from the parent rock. V, Cr, Co, Ni, Cu, Zn, Cd, and Pb are influenced by both natural and anthropogenic factors, with Cd being significantly impacted by human activities. The evaluation of soil heavy metals using the geoaccumulation index method indicates that V, Cr, Co, Ni, Cu, Zn, Zr, Ba, Hf, and Pb are non-polluted, Cd exhibits moderate pollution, and Sr shows moderately heavy pollution. From a geochemical perspective, it can be inferred that heavy metals in black shale soil are likely to be secondarily enriched in clay and iron oxide minerals.

Keywords: black shale; major elements; trace elements; weathering; heavy metal

check for updates

Citation: He, W.; Dai, D.; Ren, B.; Tang, Z.; Qiu, Y. Heavy Metal Regularity of Carboniferous Weathered Black Shale in Qiziqiao Area, Central Hunan. *Minerals* **2023**, *13*, 1044. https://doi.org/10.3390/min13081044

Academic Editors: Saglara S. Mandzhieva and Maria Economou-Eliopoulos

Received: 5 June 2023
Revised: 3 August 2023
Accepted: 4 August 2023
Published: 6 August 2023

Copyright: © 2023 by the authors. Licensee MDPI, Basel, Switzerland. This article is an open access article distributed under the terms and conditions of the Creative Commons Attribution (CC BY) license (https://creativecommons.org/licenses/by/4.0/).

1. Introduction

The state of the soil environment in China is relatively pessimistic and receiving widespread attention [1]. The 2014 National Soil Pollution Survey Report indicated that ~20 million ha of arable land in China (20% of the national total) is affected by varying degrees of heavy metal pollution. Specifically, severe heavy metal soil pollution poses a significant threat to ecological and human health alike [2–4]. Soil heavy metals are derived from two main sources: natural or anthropogenic activities [5]. Regarding human activities, many scholars have assessed the sources of heavy metals [6–10] and characteristics of soil pollution [11], conducted environmental quality surveys [12–14], and evaluated pollution

remediation [15–18]. Natural sources primarily arise from the enrichment of heavy metals contained in parent materials during soil formation due to weathering, leaching, and others, thereby forming a geological background value [19–22]. In this regard, numerous scholars have explored the activity characteristics of elements during rock weathering and soil formation through geochemical analyses of weathering profiles, as well as surface water, isotopes, and the element occurrence form [23–32]. Research has shown that black shale is uniquely rich in organic matter and sulfide minerals, which are easily weathered and decomposed when exposed to surface conditions. Foreign scholars have studied the toxicity, pollution degree, and ecological risk of heavy metals in river and lake sediments [33–37]. This natural pollution source produces acid mine drainage and leaching and releases heavy metals [38–41].

In recent years, numerous scholars have conducted research on the migration of trace elements in the process of soil formation, focusing on the interface activities, a morphological analysis, migration and transformation, and the crop adsorption of heavy metals from a soil genesis perspective. They have also investigated the influence of constant elements and oxides in soils and the relative migration of soil-indicative elements [42–49]. In addition to studying the gas content of black shale [50–52], scholars in China have conducted extensive research on the migration laws of heavy metals. They carried out chemical composition analyses of black shale at different degrees of weathering, aiming to explore the characteristics of heavy metal pollution in the corresponding black shale soils of central Hunan. Furthermore, they enacted regional elemental geochemical analyses of crops and examined the transformation and migration characteristics of heavy metals in typical farmland soils of China. Additionally, they investigated the surface geochemistry and environmental effects of selenium and heavy metals in the lower Cambrian black shale [53–56].

Previous investigations and analyses have revealed varying degrees of heavy metal contamination in the developed soils of black shale areas. However, these studies have predominantly concentrated on Cambrian black shale, leaving a gap in research regarding the migration and enrichment of heavy metals during the weathering of Carboniferous black shale.

Accordingly, based on the geochemical analysis of elements in the outcrops of black shale in the Qiziqiao area of central Hunan province, this study followed previously established research methods to explore the activity patterns of heavy metals during the weathering of regional Carboniferous black shale, thereby providing a scientific reference for further research on similar key areas.

2. Samples and Experimental Methods

2.1. Study Area Background

The Qizi (QZ) profile of the Carboniferous black shale in the central Hunan region is located near a quarry, approximately 600 m northwest of the train station in Qizi Town, Xiangxiang City (Figure 1). The black shale in the section has an outcrop thickness of 2.5 m, with no visible bottom, and is overlain by a 5.5-m-thick layer of limestone. Qizi Town is located in western Xiangxiang City, and is part of the Xiang-Gan hilly region in southern China. The region is characterized by hilly and mountainous terrain, with a higher elevation in the east and a lower elevation in the west, while the northern and southern ends also exhibit lower elevations. The highest point is Wanshan, with an altitude of 120 m. The area is characterized by abundant rainfall and a humid subtropical monsoon climate. The rivers in the area belong to the Lianshui River system, a tributary of the Xiangjiang River, and flow from west to east through the Shuifumiao Reservoir. The total area of this reservoir is 4480 ha, with a year-round capacity of 570 million m^3 [57]. The main strata in the Qiziqiao area are the Carboniferous (Zimenqiao, Ceshui, Shidengzi, Tian'eping, and Malanbian formations) and Devonian (Changlongjie–Menggongao, Xikuangshan, Shetianqiao, Qiziqiao, and Tiaomajian formations) formations, with black shale distributed in the Ceshui and Malanbian formations of the former and in the Changlongjie–Menggongao

and Shetianqiao formations of the latter. Additionally, the Qizi Town area is rich in mineral resources, with confirmed reserves of limestone (6 billion tons), dolomite (300 million tons), refractory clay (2.18 million tons), coal, and brown iron ore. The total cultivated land area is 2173 ha.

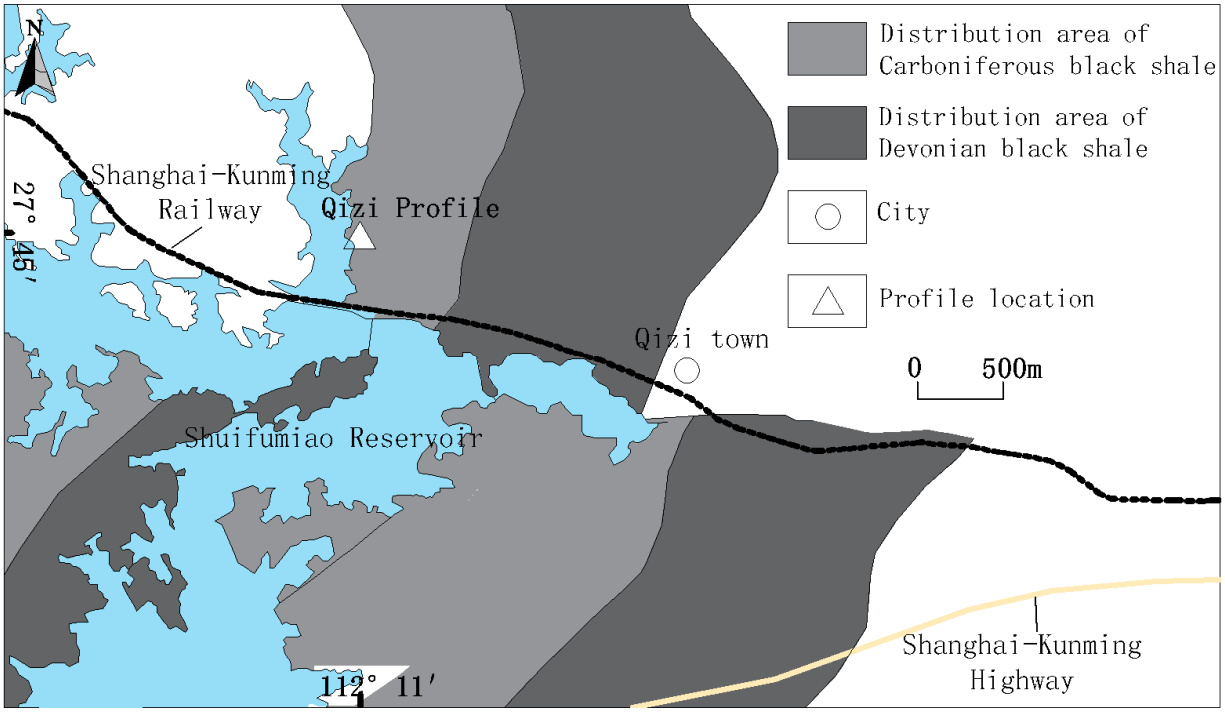


Figure 1. Geological sketches of the study area in Qizi Town.

2.2. Sample Collection and Preparation

Following field geological profile measurements, systematic sampling was conducted on the Qizi profile. The samples collected included fresh black shale, weathered black shale, and soil. In addition, individual pieces of fully weathered limestone and surface soil were collected nearby, and all nine samples were labeled as QZ. When collecting fresh black shale (FB) samples, the surface-weathered rocks were removed using a geological hammer, and deep unweathered fresh samples were collected. Middle-weathered black shale (MW) and strongly weathered black shale (SW) were sampled from the surface of the profile based on their different weathering characteristics using a geological hammer. When collecting black shale soil (BS), the surface impurities were removed, and 10 cm × 10 cm × 10 cm samples were acquired. The specific characteristics of each rock and soil sample are listed in Table 1. All samples weighed between 1.5 and 2.0 kg, and were placed in geological sample bags for transport to a laboratory.

In the lab, soil samples were placed in a drying tray, spread into a thin layer of 2–3 cm, crushed, and turned over at appropriate intervals to remove gravel, sand, and plant residues. The dried samples were then poured onto an organic glass plate for coarse grinding, and the impurities were removed and mixed uniformly. Thereafter, the samples were ground, crushed in an agate bowl, and passed through a 100-mesh nylon sieve. Rock samples were dried in an oven at 120 °C, crushed, and passed through a 60-mesh sieve to obtain a powdered sample. Then, 5.0 g of the powdered sample was taken and ground using an agate mortar before being passed through a 200-mesh sieve for subsequent major- and trace-element analyses. The samples were prepared as follows: 0.1–0.2 g of the sieved sample was weighed. The samples were placed in a digestion tank, and 1 mL of hydrochloric acid, 4 mL of nitric acid, 1 mL of hydrofluoric acid, and 1 mL of hydrogen peroxide were digested using a microwave digestion device. Following digestion, samples were cooled to room temperature, the lid of the digestion tanks was carefully opened,

and the tanks were then placed in an acid-evaporating instrument to evaporate at 150 °C until the internal solution was nearly dry. After cooling to room temperature, the internal solution was dissolved in deionized water. The solution was then transferred to a 50 mL volumetric flask, and the volume was raised to 50 mL with deionized water.

Table 1. Apparent characteristics of rock and soil samples in Qizi profile.

Sample	Weathering Degree and Type	Apparent Characteristics
QZ-1	Fresh black shale (FB)	Appears black, well-developed bedding, relatively intact rock, feels heavy when held.
QZ-2	Fresh black shale (FB)	
QZ-3	Fresh black shale (FB)	
QZ-4	Moderately weathered black shale (MW)	Contains yellowish-white weathering products, locally visible bedding, fragmented rock, feels light when held.
QZ-5	Strongly weathered black shale (SW)	Light-yellow weathering products, original rock structure disappeared, highly fragmented rock.
QZ-6	Black shale soil (BS)	Dark brownish-black color, loose soil texture, visible small amount of plant roots and shale debris.
QZ-7	Black shale soil (BS)	
QZ-8	Weathered limestone soil	Reddish-brown color, contains a small amount of gravel, slightly moist and moderately dense, uneven soil texture.
QZ-9	Surface soil of limestone	Reddish-brown gravelly soil, slightly moist and moderately dense, uneven soil texture, visible small amount of plant roots.

2.3. Sample Analysis

The major and trace elements in the black shale and soil samples were analyzed at the Testing Center of the Hunan Institute of Geology. A ZSX Primus IV wavelength-dispersive X-ray fluorescence (XRF) spectrometer was used for the analysis of major elements, lithophilic elements (Sr and Ba), and high-field-strength elements (Zr and Hf). The detection limits of SiO_2, Al_2O_3, Fe_2O_3, K_2O, Na_2O, CaO, and MgO are 0.27, 0.07, 0.05, 0.05, 0.09, and 0.05%, respectively. The detection limits of P, Ti, Mn, Sr, Ba, Zr, and Hf are 10.0, 50.0, 10.0, 2.0, 11.7, 2.0, and 1.7 $mg \cdot kg^{-1}$, respectively. The heavy metal elements V, Cr, Co, Ni, Cu, Zn, Cd, and Pb examined in the present study were analyzed using an iCAP Q inductively coupled plasma mass spectrometer. When the sample size was 0.1 g, the detection limits of the eight metal elements ranged from 0.4 to 3.2 $mg \cdot kg^{-1}$, whereas the determination limits ranged from 1.6 to 12.8 $mg \cdot kg^{-1}$. Before measurement, the solution was run through a filter membrane or the supernatant was collected for measurement. A blank sample was prepared using the same steps and reagents as those for sample preparation. A minimum of two blank samples were analyzed for each batch of samples.

3. Results and Analysis

3.1. Major Elements

The major elemental analyses' results of the Carboniferous black shale and soil samples from central Hunan are shown in Table 2, while the variation characteristics are presented in Figure 2. Overall, the content of major elements, such as SiO_2, Al_2O_3, Fe_2O_3, K_2O, and TiO_2 increased with the degree of weathering the black shale samples to soil. The CaO content and burning loss (LOI) decreased with the degree of weathering as well, whereas they decreased dramatically from highly weathered black shale to soil. The MnO and P_2O_5 content remained relatively stable at low levels throughout weathering and were significantly enriched in the soil. The MgO content oscillated and was substantially enriched in the soil, while the Na_2O content displayed an overall decrease. Compared with the adjacent limestone surface soil, the SiO_2, Al_2O_3, Fe_2O_3, Na_2O, P_2O_5, and TiO_2 content of the black shale soil was roughly identical, whereas the CaO, MgO, K_2O, MnO, and LOI content was much higher than that of the limestone surface soil. The differences in chemical composition among black shales with different degrees of weathering are likely the result of weathering, while the sharp increases or decreases in major elements in black

shale soil may have resulted from the soil formation process, and are deserving of further attention.

Table 2. Solid content of major elements in weathered and unweathered black shales from the Qizi profile in central Hunan, China (wt%).

Species	QZ-1	QZ-2	QZ-3	QZ-4	QZ-5	QZ-6	QZ-7	QZ-8	QZ-9
SiO_2	21.11	22.23	22.42	25.93	27.45	42.17	45.62	69.54	63.73
Al_2O_3	4.92	4.86	5.16	7.51	9.13	16.59	16.99	19.88	18.03
Fe_2O_3	1.40	1.42	1.41	1.61	1.82	4.94	5.26	6.95	6.36
CaO	38.42	39.06	38.52	34.06	32.09	14.08	15.02	0.61	0.55
MgO	0.86	0.87	0.86	0.81	0.86	1.42	1.48	0.44	0.43
K_2O	0.56	0.54	0.54	0.94	1.18	2.34	2.37	1.38	1.27
Na_2O	0.33	0.34	0.31	0.43	0.49	0.39	0.35	0.36	0.38
MnO	0.03	0.03	0.03	0.03	0.03	0.06	0.06	0.03	0.03
P_2O_5	0.02	0.02	0.02	0.02	0.02	0.06	0.05	0.05	0.05
TiO_2	0.21	0.22	0.20	0.30	0.36	0.71	0.67	0.96	1.00
LOI	31.18	32.42	30.96	28.29	27.34	16.87	16.33	5.96	5.10
CIA	74.39	74.03	76.26	75.52	75.94	81.27	82.02	88.11	87.28
ICV	8.49	8.73	8.11	5.08	4.03	1.44	1.48	0.54	0.55

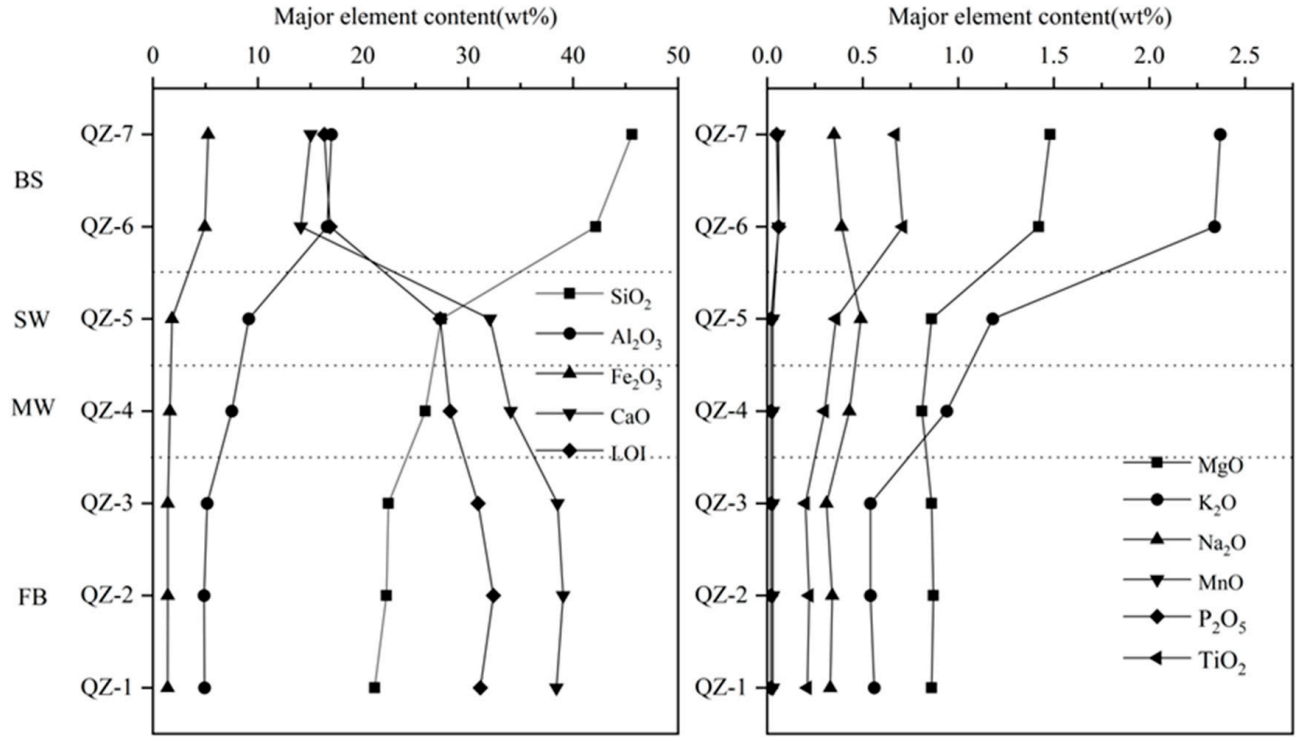


Figure 2. The variation characteristics of major element content with weathering degree.

3.2. Trace Elements

The trace element analysis results of Carboniferous black shale and soil samples in central Hunan are shown in Table 3. The 12 trace elements examined belong to a broad category of heavy metals based on their atomic densities (>4.5 g·cm^{-3}) [58]. In this study, these elements were further classified into heavy metals (Cd, Cu, Pb, Cr, Zn, Ni, V, and Co), lithophiles (Sr and Ba), and high-field-strength elements (Zr and Hf). Trace element content varied greatly with the degree of black shale coal series weathering. The enrichment coefficient K_i (the concentration of the trace element relative to the background value of the reference element) was used to evaluate the enrichment characteristics of the trace elements, where K_i values > 1.0 and <1.0 indicate relative enrichment and depletion, respectively.

The reference background values for rocks in this study include the world average shale (WAS) [59], the eastern Chinese upper crust (CEUC), and the lower Cambrian black shale in central Hunan (LCBS). The reference background values for the soil include the Chinese average soil (CAS), Hunan average soil (HNAS), and black shale soil from the lower Cambrian period in central Hunan (LCBSS; Table 4). Figure 3 presents a standardized diagram of the relative values for fresh black shale (reference rock value) and black shale soil (reference soil value). Figure 4 is a standardized diagram of heavy metal elements in black shale at different weathering degrees relative to bedrock. The distribution characteristics of heavy metals, lithophiles, and high-field-strength elements with the degree of weathering of the Carboniferous black shale in central Hunan is summarized in the subsequent subsections.

Table 3. Solid content of trace elements in weathered and unweathered black shales from the Qizi profile in central Hunan, China (ppm).

Species	QZ-1	QZ-2	QZ-3	QZ-4	QZ-5	QZ-6	QZ-7	QZ-8	QZ-9
V	25	40	30	37	46	120	140	134	121
Cr	27	46	34	41	52	94	109	97	82
Co	3	5	5	5	6	13	15	19	13
Ni	12	18	16	17	20	42	48	57	37
Cu	10	14	12	13	15	29	35	35	33
Zn	27	25	28	25	29	88	88	140	98
Sr	395	310	317	324	309	249	285	42	39
Zr	84	95	124	100	99	159	149	222	234
Cd	0.2	0.2	0.2	0.1	0.2	0.7	0.5	1.3	0.2
Ba	65	96	74	66	119	252	281	224	208
Hf	2.1	2.5	3.1	2.6	2.5	4.4	4.2	6.4	6.6
Pb	10	13	11	11	14	37	32	33	30

Table 4. Heavy metal content in rocks and soils from different regions (ppm).

Background Value	V	Cr	Co	Ni	Cu	Zn	Sr	Zr	Cd	Ba	Hf	Pb
Rocks												
WAS	130	90	19	68	45	95	300	160	0.3	581	2.8	20
CEUC	70	44	12	21	17	63	300	170	0.075	640	4.8	18
LCBS	976	146	16	60	84	98	416	100	0.6	4101	2.8	37
Soils												
HNAS	105.4	71.4	14.6	31.9	27.3	94.4	44	183	0.1	383	9.2	29.7
CAS	82.4	61	12.7	26.9	22.6	74.2	167	256	0.1	469	7.8	26
LCBSS	573.7	143.7	21.9	53.3	88.5	118.1	60.4	225	0.7	1920.1	6.3	47.9

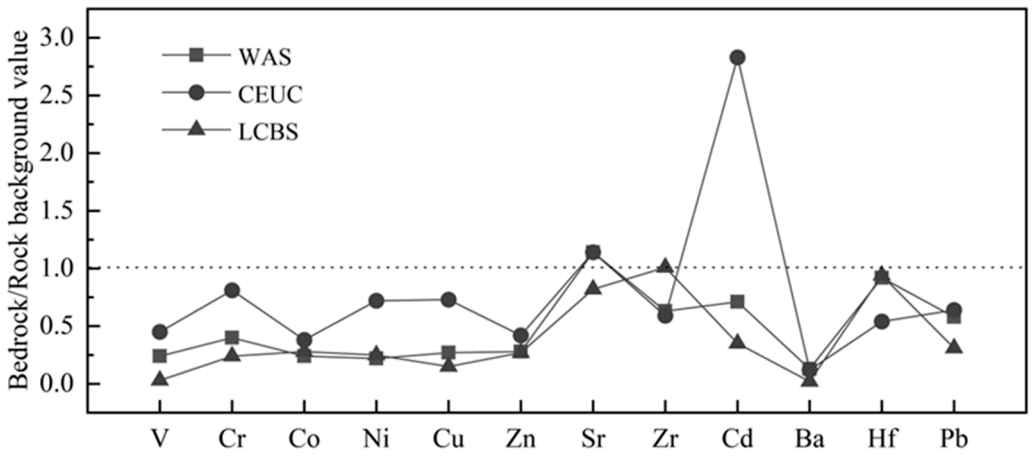


Figure 3. *Cont.*

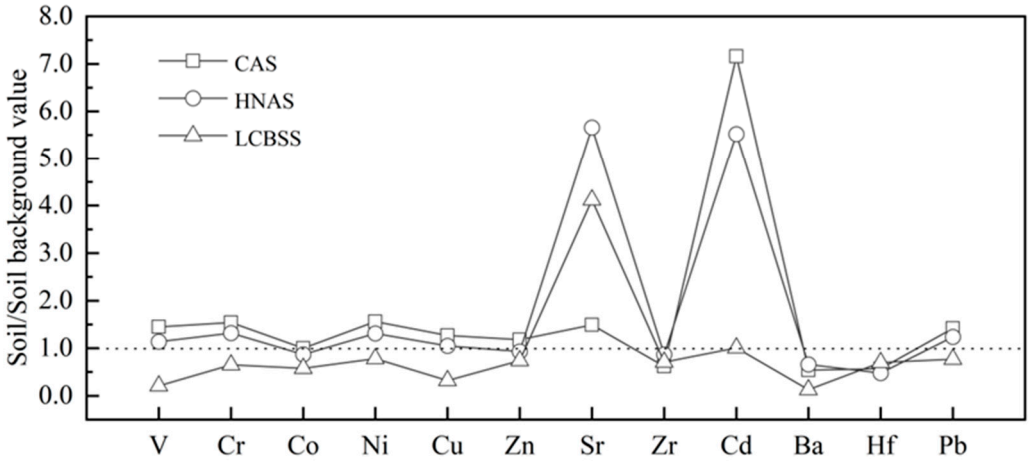


Figure 3. The standardized diagram of heavy metal elements in bedrock and soil of the Qizi profile.

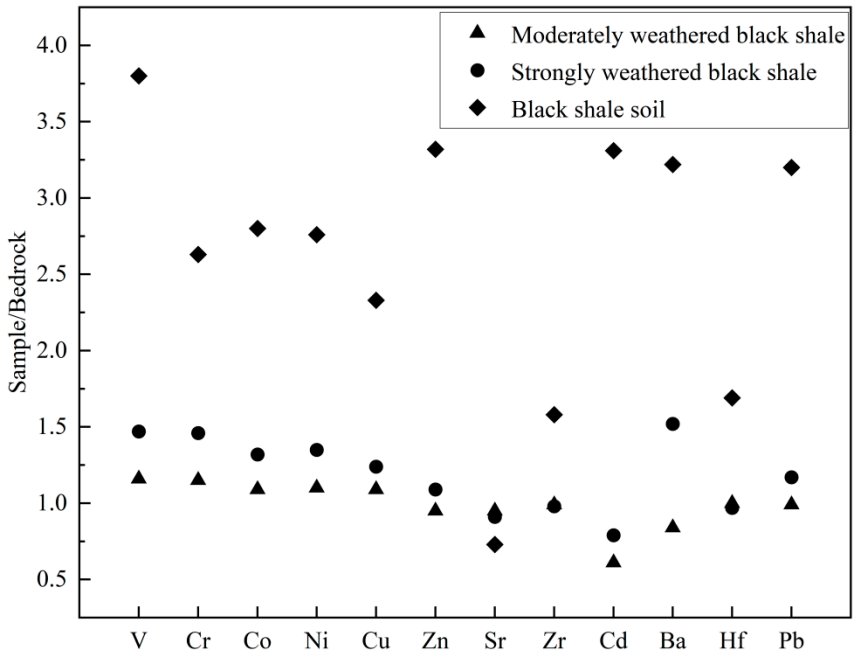


Figure 4. Standardized diagram of weathered black shale relative to bedrock.

3.2.1. Heavy Metals

The content of the eight heavy metals (V, Cr, Co, Ni, Cu, Zn, Cd, and Pb) in fresh black shale from the QZ section was 31.51, 35.7, 4.54, 15.18, 12.33, 26.4, 0.21, and 11.52 mg·kg^{-1}, respectively. Compared to world shale, the QZ section black shale from the Carboniferous system in central Hunan showed an obvious deficit in these eight heavy metals, particularly V, Cr, Co, Ni, Cu, and Zn, all with K_i values < 0.5. Compared to the upper crust of eastern China, with the exception of Cd (which displayed an obvious enrichment, K_{Cd} = 2.83), the enrichment features of other heavy metals were similar to those of world shales, showing either no enrichment feature (K_i < 1), or an obvious deficit (K_i = 0.5). Compared to the lower Cambrian black shale in central Hunan, the enrichment coefficients of these heavy metals were all <0.35, indicating that the overall abundance of the eight heavy metals of the Carboniferous black shale in central Hunan was lower than that in the lower Cambrian black shale.

The enrichment characteristics of heavy metals during the weathering of black shale (excluding weathered soil) were not evident, with enrichment factors relative to the average value of the bedrock ranging from K_i = 0.61 to 1.47; however, the enrichment factors of the heavily weathered black shale were all greater than those of the weakly weathered black

shale. In the black shale soils of the QZ profile, the content of heavy metal elements was higher than that of the Chinese soil background value, among which the enrichment characteristics of Cr, Ni, and Cd were the most obvious (K_i = 1.54, 1.56, and 7.16, respectively, for samples taken from QZ-6). Relative to the soil background value in Hunan, the enrichment characteristics of all other heavy metal elements were less obvious (K_i = 0.87~1.32), with the exception of Cr, which displayed a significant enrichment (K_i = 5.52). Compared with the lower Cambrian black shale soils in central Hunan, these heavy metals showed patterns of depletion, although their content remained far higher than that of the bedrock.

3.2.2. Compatible Trace Elements

The content of compatible trace elements Sr and Ba in fresh black shale of the QZ profile was 340.53 mg·kg^{-1} and 78.11 mg·kg^{-1}, respectively. The Sr content was slightly higher than the world shale background value and the upper continental crust of China, with K_{Sr} = 1.14, whereas Ba showed apparent depletion features, with K_{Ba} = 0.13 and 0.12, respectively. The K_{Sr} relative to the lower Cambrian black shale was 0.82, and was notably insignificant, while Ba showed a severe depletion feature (K_{Ba} = 0.02).

The relative enrichment coefficients of Sr to bedrock in the weakly weathered, moderately weathered, and soil samples were 0.95, 0.91, and 0.78, respectively, indicating decreasing patterns with increasing degrees of weathering. Although Sr in the black shale soil was depleted relative to the bedrock, it was significantly enriched relative to the background values of the Chinese and Hunan soils, with K_{Sr} = 1.49 and 5.66, respectively. Compared with the lower Cambrian black shale soil in central Hunan, it also exhibited obvious enrichment characteristics (K_{Sr} = 4.12). The relative enrichment coefficients of Ba in the bedrock were 0.84, 1.52, and 3.41, respectively, indicating significantly enriched patterns with increasing degrees of weathering; however, values remained depleted relative to the background levels of the lower Cambrian Chinese, Hunan, and black shale soils in central Hunan.

3.2.3. High-Field-Strength Elements

The content of Zr and Hf in fresh black shale from the QZ profile was 100.82 mg·kg^{-1} and 2.59 mg·kg^{-1}, respectively. The enrichment characteristics relative to the global shale background and upper continental crust in eastern China were not obvious; however, K_i = 0.54~0.92. Compared with lower Cambrian black shale in central Hunan, the two were roughly equal (K_{Zr} and K_{Hf} of 1.01 and 0.94, respectively). The enrichment characteristics of Zr and Hf relative to the bedrock were not obvious during weathering wither ($K_i \approx 1$); but, they were also significantly enriched in black shale soil (K_{Zr} and K_{Hf} of 1.53 and 1.66, respectively). Their content, however, was still lower than the background values of lower Cambrian black shale soil in central Hunan.

The heavy metals in the above-mentioned Carboniferous black shale were significantly enriched (except for Sr) in weathered soils, showing geochemical characteristics of low background values and a high enrichment. The enrichment features of various trace elements at different weathering degrees were also distinct, indicating that trace elements have complex chemical activities throughout the weathering process of black shale.

4. Discussion

4.1. Activity Patterns of Heavy Metal Elements

4.1.1. Migration and Redistribution of Heavy Metal Elements

To reveal the migration and redistribution of various elements throughout the process of black shale weathering, it was necessary to calculate the mass transfer coefficients of each element. A mass transfer coefficient is an effective indicator for characterizing the activity of elements. Previous studies have shown that Ti, Zr, and Nb are primarily enriched in weathering-resistant secondary minerals with a weak mobility and difficult leaching capacity. Similarly, Hf, Ta, and other high-field-strength elements are relatively stable in chemical activity, and can be considered as inert elements that do not undergo obvious

leaching migration during soil formation processes. Accordingly, these metals are often used as reference elements in mass-balance calculations. Trace element analysis results showed that the Zr content in the sample was relatively high and exhibited a small degree of variation; therefore, Zr was selected as the reference element in this study. The τ value is calculated using Equation (1):

$$\tau = \frac{C_{X,S}/C_{Zr,S}}{C_{X,B}/C_{Zr,B}} - 1 \quad (1)$$

where $C_{X,S}$ and $C_{Zr,S}$ are the content of elements X and Zr in the sample, respectively, while $C_{X,B}$ and $C_{Zr,B}$ are the content of elements X and Zr in the bedrock, respectively. When $\tau > 0$, <0, or =0, element X was enriched, depleted, or did not migrate, respectively [60].

The average elemental content of three fresh black shale samples (QZ-1, QZ-2, and QZ-3) was used for the mass balance calculations, and Figure 5 presents a diagram of the mass transfer coefficients for the trace elements in the weathering profile of black shale.

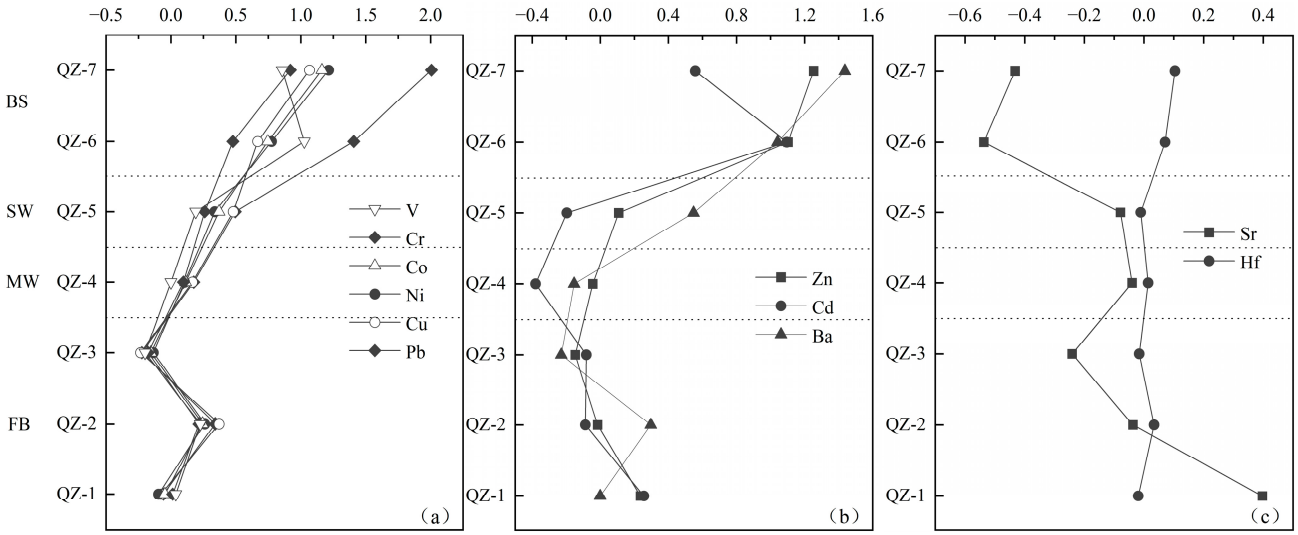


Figure 5. Diagram of mass transfer coefficients of trace elements during weathering process of black shale in the Qizi profile. With the weathering of black shale: (**a**) relative enrichment; (**b**) both enrichment and loss; (**c**) loss (Sr) or almost no migration (Hf).

The τ_{ij} values of V, Cr, Co, Ni, and Cu in the QZ profile gradually increased from fresh to moderately weathered, to strongly weathered black shale, and to black shale soil, with changes of 0.020 → 0.176 → 0.495 → 1.708, 0.020 → 0.165 → 0.480 → 0.867, 0.009 → 0.104 → 0.337 → 0.994, 0.013 → 0.113 → 0.370 → 0.954, and 0.018 → 0.096 → 0.260 → 0.698, respectively. The τ_{ij} value of Pb also increased with the degree of weathering, changing (0.020 → 0.000 → 0.191 → 0.942) along this weathering gradient. The τ_{ij} values of these heavy metals were all > 0, indicating that they were not generally leached out during weathering, but may have been relatively enriched or undergone secondary enrichment. For example, Al can replace V in a homologous manner in clay minerals, and with Fe in manganese (hydro) oxides during the weathering of black shale [61]. A Pearson's correlation analysis of the main trace metals in the QZ profile (Table 5) showed that V, Cr, Ni, and Cu were all significantly positively correlated, indicating that they had similar sources and geochemical behaviors.

Table 5. The Pearson correlation coefficients for major and trace elements of samples from the Qizi profile.

	V	Cr	Ni	Cu	Zn	Sr	Zr	Cd	Ba	Hf	Pb	Al_2O_3	Fe_2O_3
V	1												
Cr	0.994 **	1											
Ni	0.999 **	0.995 **	1										
Cu	0.997 **	0.993 **	0.998 **	1									
Zn	0.981 **	0.956 **	0.975 **	0.968 **	1								
Sr	−0.736	−0.773 *	−0.756 *	−0.73	−0.697	1							
Zr	0.879 **	0.856 *	0.888 **	0.872 *	0.910 **	−0.824 *	1						
Cd	0.872 *	0.833 *	0.863 *	0.840 *	0.943 **	−0.687	0.903 **	1					
Ba	0.993 **	0.990 **	0.993 **	0.988 **	0.976 **	−0.742	0.873 *	0.882 **	1				
Hf	0.924 **	0.903 **	0.930 **	0.918 **	0.943 **	−0.824 *	0.993 **	0.913 **	0.914 **	1			
Pb	0.964 **	0.950 **	0.960 **	0.944 **	0.983 **	−0.784 *	0.912 **	0.959 **	0.966 **	0.942 **	1		
Al_2O_3	0.972 **	0.969 **	0.971 **	0.961 **	0.960 **	−0 0.745	0.865 *	0.861 *	0.966 **	0.899 **	0.952 **	1	
Fe_2O_3	0.993 **	0.975 **	0.989 **	0.983 **	0.996 **	−0.71	0.895 **	0.912 **	0.985 **	0.934 **	0.977 **	0.977 **	1

* denotes significance at $p < 0.05$; ** denotes significance at $p < 0.01$.

The τ_{ij} values of Zn, Cd, and Ba were both positive and negative, indicating that both enrichment and depletion occurred throughout the weathering process with high activity; however, in the black shale soil, τ_{ij} values of these three elements were positive (reaching 1.178, 0.827, and 1.239), indicating that they had undergone relative enrichment during the soil formation process. These three elements also had a significantly positive correlation ($R_{Zn\text{-}Cd}$ = 0.943, $R_{Zn\text{-}Ba}$ = 0.976, and $R_{Cd\text{-}Ba}$ = 0.882), further supporting their shared origin.

The τ_{ij} values of Sr were generally <0, indicating that the element tended to leach out during the weathering process via its strong mobility. This is notably similar to the behavior of Sr in the lower Cambrian black shale during weathering. Generally, Sr exists widely in carbonate and silicate minerals, substituting for Ca and Mg via isomorphic substitution. As weathering progressed, the decomposition of minerals (e.g., calcite and plagioclase) promoted the leaching of Sr.

The τ_{ij} values of Hf largely fell between −0.1 and 0.1, indicating a weak mobility, and almost no migration during weathering or soil formation processes. This is likely because this element mainly exists in accessory minerals (e.g., monazite and zircon), which maintain a strong weathering resistance.

4.1.2. Enrichment Factor Analysis

The enrichment factor method is an important indicator for quantitatively assessing the degree of element enrichment. The calculation formula is given using Equation (2):

$$EF = (C_i/C_n)_S/(C_i/C_n)_{RBS} \quad (2)$$

In Equation (2), EF represents the enrichment factor for element i, C_i denotes the solid content of element i in the sample or the background value of element i in the soil, and C_n represents the solid content of the reference element in the sample or the background value of the reference element in the soil. In this study, Zr was chosen as the reference element. The soil background value was selected as HNAS. When EF < 1, it is considered non-enriched; when $1 \leq EF < 2$, it is mildly enriched; when $2 \leq EF < 5$, it is moderately enriched; when $5 \leq EF < 20$, it is heavily enriched; when $20 \leq EF < 40$, it is severely enriched; and when $EF \geq 40$, it is extremely enriched [62].

According to Table 6, the fresh black shale samples from the QZ profile exhibit no significant enrichment characteristics for heavy metals V, Cr, Co, Ni, Cu, Zn, and Pb (EF < 1.0). However, Cd shows a moderate enrichment with an enrichment factor (EF) of 3.11. The lithophile element Sr demonstrates a heavy enrichment (EF = 14.61), while Ba shows no significant enrichment. The high-field-strength element Hf does not exhibit any enrichment. In different degrees of weathered black shale, the heavy metals V, Co, Zn, and Pb also show no enrichment (EF < 1.0). Cr, Ni, and Cu display a mild enrichment in highly weathered black shale ($1 \leq EF < 2$). Cd exhibits a mild enrichment (EF = 1.88) in moderately weathered shale and a moderate enrichment (EF = 2.43) in highly weathered shale. The enrichment factor for the lithophile element Sr slightly decreases with increasing

weathering, but it still reaches a heavy enrichment level ($5 \leq EF < 20$). Ba and the high-field-strength element Hf do not show significant enrichment during the weathering process ($EF < 1.0$). In black shale soils, except for Ba and Hf, all other heavy metals show some degree of enrichment. Sr and Cd exhibit a heavy enrichment, with enrichment factors of 7.24 and 5.53, respectively. In summary, it can be inferred that the heavy metals Ba and Hf in black shale soil originate from the parent rock. Although the element Sr shows a high degree of enrichment in the soil, its enrichment factor decreases with increasing weathering, indicating a natural source. V, Cr, Co, Ni, Cu, Zn, Cd, and Pb are influenced by both natural and anthropogenic factors, with Cd being significantly influenced by human activities, possibly associated with mining activities.

Table 6. Enrichment factors during weathering processes of QZ profile black shale.

Species	V	Cr	Co	Ni	Cu	Zn	Sr	Cd	Ba	Hf	Pb
QZ-1	0.51	0.84	0.51	0.82	0.83	0.63	19.62	3.80	0.37	0.50	0.73
QZ-2	0.73	1.24	0.71	1.07	1.00	0.50	13.53	2.76	0.48	0.53	0.86
QZ-3	0.42	0.70	0.49	0.73	0.68	0.43	10.67	2.78	0.29	0.50	0.56
Average	0.55	0.93	0.57	0.88	0.83	0.52	14.61	3.11	0.38	0.51	0.72
QZ-4	0.64	1.06	0.62	0.96	0.90	0.49	13.48	1.88	0.31	0.52	0.70
QZ-5	0.81	1.34	0.75	1.18	1.03	0.56	12.94	2.43	0.57	0.51	0.84
QZ-6	1.31	1.51	1.00	1.51	1.21	1.07	6.50	6.34	0.76	0.55	1.43
QZ-7	1.63	1.88	1.25	1.87	1.57	1.14	7.97	4.71	0.90	0.57	1.31
Average	1.47	1.69	1.13	1.69	1.39	1.11	7.24	5.53	0.83	0.56	1.37

4.2. Mechanisms of Soil Heavy Metal

Monitoring the occurrence of heavy metals in soil is crucial for understanding the development and trends of correlated pollution, as well as for managing the prevention and control of these processes. Factors such as soil pH and organic matter content can affect the heavy metals in soil. Previous studies have generally used sequential extraction methods to determine the occurrence of heavy metals in soil; thus, the present study attempted to explore the occurrence characteristics of heavy metals in shale soil from a geochemical perspective.

The major elemental analysis showed that the chemical composition of Carboniferous black shale soil was characterized by low Na, and high Al and Fe; therefore, the geochemical behaviors of Al_2O_3 and Fe_2O_3 throughout the weathering of the black shale may underscore the main factors determining the occurrence of heavy metals in these soils. A significant correlation was observed between Al_2O_3, Fe_2O_3, and the other trace elements (Table 5). During black shale weathering, the activity of trace elements is controlled by their host minerals. For example, the secondary enrichment of V may occur during the weathering of black shale, which is controlled by clay minerals and iron–manganese (hydro)oxides, as V can replace Al in the former and Fe in the latter through isomorphic substitution [61].

The Chemical Index of Alteration (CIA) and Index of Composition Variability (ICV) of the Carboniferous black shale (QZ profile) samples across various degrees of weathering are listed in Table 2. The CIA values increased with the degree of weathering, from fresh black shale to moderately weathered, to strongly weathered, and to black shale soil, with averages of 74.90, 75.52, 75.94, and 81.65, respectively, thereby indicating the transformation of feldspar into clay minerals. Alternatively, the average ICV values were 8.45, 5.08, 4.03, and 1.46, respectively. Although all values were >1, they decreased significantly with an increasing weathering degree, indicating that the unaltered minerals decreased, and the clay minerals increased due to secondary processes.

Previous studies have shown that the sediment grain size can affect the solid content of heavy metals. Coarse-grained samples (<2 mm) often contain a large number of rock structural substances such as quartz, in which the solid content of heavy metals is often low [63]. Conversely, fine-grained samples are typically composed of clay minerals with, commonly, a high heavy metal content for solids [64]. Accordingly, the major elemental

compositions of rocks reflect their primary mineral compositions; thus, it can be inferred that heavy metals in black shale soils mainly exist in clay and iron oxide minerals.

4.3. Assessment of Heavy Metal Pollution in Soil

In this study, the geoaccumulation index (I_{geo}) method was used to assess heavy metal pollution. The calculation formula for I_{geo} is given using Equation (3):

$$I_{geo} = \log_2[C_i/(B_i \times k)] \quad (3)$$

In Equation (3), I_{geo} represents the geoaccumulation index, C_i is the solid content of the evaluated element i in the soil, and B_i is the environmental background value for element i, which was selected as the soil background value in Hunan (HNAS) in this study. The factor k accounts for variations in the background value due to diagenetic processes and is typically taken as 1.5. Müller [65] classified the geoaccumulation index into seven levels: $I_{geo} < 0$, $0 \leq I_{geo} < 1$, $1 \leq I_{geo} < 2$, $2 \leq I_{geo} < 3$, $3 \leq I_{geo} < 4$, $4 \leq I_{geo} < 5$, and $I_{geo} \geq 5$. The corresponding pollution levels are categorized as non-pollution, slight pollution, moderate pollution, moderately heavy pollution, heavy pollution, severe pollution, and extremely heavy pollution.

The results of the geoaccumulation index analysis are presented in Table 7. From the table, it can be observed that, in the soil of the QZ profile black shale, except for Sr and Cd elements, there is no pollution of other heavy metal elements, as indicated with geoaccumulation index values less than 0, primarily originating from natural sources. Cd exhibits a moderate pollution level (I_{geo} = 1.62), influenced by both natural and anthropogenic sources. Sr shows a moderately heavy pollution level (I_{geo} = 2.01).

Table 7. Geoaccumulation index of heavy metals in soil from the QZ profile.

Species	QZ-6	QZ-7	Average	Pollution level
V	−0.40	−0.18	−0.29	Non-pollution
Cr	−0.19	0.02	−0.08	Non-pollution
Co	−0.78	−0.56	−0.67	Non-pollution
Ni	−0.19	0.02	−0.09	Non-pollution
Cu	−0.51	−0.23	−0.37	Non-pollution
Zn	−0.69	−0.69	−0.69	Non-pollution
Sr	1.91	2.11	2.01	Moderately heavy pollution
Zr	−0.79	−0.88	−0.83	Non-pollution
Cd	1.88	1.35	1.62	Moderate pollution
Ba	−1.19	−1.03	−1.11	Non-pollution
Hf	−1.65	−1.71	−1.68	Non-pollution
Pb	−0.27	−0.50	−0.38	Non-pollution

5. Conclusions

(1) The content of heavy metals (including V, Cr, Co, Ni, Cu, Zn, Cd, Ba, and Pb) in the bedrock was much lower than the background values of lower Cambrian black shale in central Hunan, whereas that of other elements, such as Sr, Zr, and Hf was roughly equal. These findings are similar to the results of the world-average shale and the eastern Chinese upper crust; however, Cd was significantly enriched relative to the upper crust of eastern China (K_{Cd} = 2.83).

(2) From fresh black shale to moderately and strongly weathered black shale, the heavy metals of V, Cr, Co, Ni, Cu, Zn, Cd, and Pb showed a slight enrichment. Comparatively, high-field-strength elements, such as Zr and Hf, showed a slight depletion; although, the enrichment features were not obvious, as the lithophile element Ba was enriched, while Sr was depleted. Save for Sr, all other elements were significantly enriched in the black shale soil, with a solid content much higher than that in the bedrock, thereby indicating the geochemical characteristics of a low background and high enrichment.

(3) The content of heavy metal elements, including V, Cr, Co, Ni, Cu, Zn, Sr, Cd, and Pb in black shale soil, was all higher than the background values of Chinese soils (similar results were obtained relative to the background values of Hunan soils, save for Co and Zn). This was particularly true for Cd, which was 7.16 times higher than that of lower Cambrian black shale soil in central Hunan. Sr was also significantly enriched (4.12 times), while Cr was relatively constant. Alternatively, the depletion characteristics of all other elements were obvious.

(4) The enrichment factor analysis of black shale at different weathering degrees reveals that the heavy metals Ba, Hf, and Sr in black shale soil originate from the parent rock. V, Cr, Co, Ni, Cu, Zn, Cd, and Pb are influenced by both natural and anthropogenic factors, with Cd being significantly influenced by human activities, possibly associated with mining activities.

(5) The evaluation of soil heavy metals using the geoaccumulation index method indicates that, except for Sr and Cd elements, other heavy metal elements show no pollution with geoaccumulation index values below 0, primarily originating from natural sources. Cd is moderately polluted (I_{geo} = 1.62), influenced by both natural and anthropogenic sources. Sr exhibits moderately heavy pollution (I_{geo} = 2.01).

(6) Based on the correlation analysis of major and trace elements in the QZ profile and the variation characteristics of major elements with weathering, CIA, and ICV, it was inferred that the heavy metals in black shale soil were largely secondarily enriched in clay and iron oxide minerals (except for Sr, which was depleted).

Author Contributions: Conceptualization, B.R.; Methodology, W.H. and D.D.; Software, W.H.; Validation, W.H., D.D. and B.R.; Formal analysis, W.H.; Investigation, W.H., D.D., B.R., Z.T. and Y.Q.; Resources, D.D. and B.R.; Data curation, W.H. and D.D.; Writing—original draft, W.H.; Writing—review and editing, D.D. All authors have read and agreed to the published version of the manuscript.

Funding: This work was supported by the National Natural Science Foundation of China (41973078), Key R&D project of Science and Technology Department of Hunan Province (2022SK2073), and Hunan Provincial Natural Science Foundation of China (Grant No. 2021JJ30242).

Data Availability Statement: The data that support the findings of this study are available from the corresponding author, Deqiu Dai, upon reasonable request.

Acknowledgments: We are very grateful for the valuable comments from three anonymous reviewers and from the journal editors, which have greatly improved the quality of this paper.

Conflicts of Interest: The authors declare no conflict of interest.

References

1. He, B.; Yun, Z.; Shi, J.; Jiang, G. Research progress of heavy metal pollution in China: Sources, analytical methods, status, and toxicity. *Chin. Sci. Bull.* **2013**, *58*, 134–140.
2. Zhang, Y.; Xiang, Y.; Yu, G.; Yuan, K.; Wang, X.; Mo, H. Classification of environmental disaster in Hunan Province. *Disaster Adv.* **2012**, *5*, 1756–1759.
3. Luo, X.; Ren, B.; Hursthouse, A.S.; Thacker, J.R.; Wang, Z. Soil from an abandoned manganese mining area (Hunan, China): Significance of health risk from potentially toxic element pollution and its spatial context. *Int. J. Environ. Res. Public Health* **2020**, *17*, 6554. [CrossRef] [PubMed]
4. Hou, H.; Shao, L.; Wang, S.; Xiao, Z.; Wang, X.; Li, Z.; Mu, G. Influence of depositional environment on coalbed methane accumulation in the Carboniferous-Permian coal of the Qinshui Basin, northern China. *Front. Earth Sci.* **2019**, *13*, 535–550. [CrossRef]
5. Lv, J.; Liu, Y.; Zhang, Z.; Dai, J. Factorial kriging and stepwise regression approach to identify environmental factors influencing spatial multi-scale variability of heavy metals in soils. *J. Hazard. Mater.* **2013**, *261*, 387–397. [CrossRef]
6. Zhang, Y.; Huang, F. Indicative significance of the magnetic susceptibility of substrate sludge to heavy metal pollution of urban lakes. *Sci. Asia* **2021**, *47*, 374. [CrossRef]
7. Jiang, F.; Ren, B.; Hursthouse, A.; Deng, R.; Wang, Z. Distribution, source identification, and ecological-health risks of potentially toxic elements (PTEs) in soil of thallium mine area (southwestern Guizhou, China). *Environ. Sci. Pollut. Res.* **2019**, *26*, 16556–16567. [CrossRef]

8. Peng, J.; Wang, C.; Li, Y.; Hu, A.; Lu, Y.; Chen, X. Geochemical characteristics and Sm-Nd geochronology of scheelite in the Baojinshan ore district, central Hunan. *Acta Petrol. Sin.* **2021**, *37*, 665–682.
9. Saydam Eker, Ç. Geochemistry and Pb isotopic proof for sources of heavy metal (loid) s in Late Cretaceous sandstones from Eastern Pontides (NE Turkey). *Environ. Earth Sci.* **2021**, *80*, 477. [CrossRef]
10. Proshad, R.; Kormoker, T.; Al, M.A.; Islam, M.S.; Khadka, S.; Idris, A.M. Receptor model-based source apportionment and ecological risk of metals in sediments of an urban river in Bangladesh. *J. Hazard. Mater.* **2022**, *423*, 127030. [CrossRef]
11. Alloway, B.J. *Heavy Metals in Soils: Trace Metals and Metalloids in Soils and Their Bioavailability*; Springer Science & Business Media: Dordrecht, The Netherlands, 2012; Volume 22.
12. Yang, W.; Deng, M.; Tang, J.; Jin, R. On the use of Markov chain models for drought class transition analysis while considering spatial effects. *Nat. Hazards* **2020**, *103*, 2945–2959. [CrossRef]
13. Deng, Q.; Qin, Y.; Ahmad, N. Relationship between Environmental Pollution, Environmental Regulation and Resident Health in the Urban Agglomeration in the Middle Reaches of Yangtze River, China: Spatial Effect and Regulating Effect. *Sustainability* **2022**, *14*, 7801. [CrossRef]
14. Pellinen, V.; Cherkashina, T.; Gustaytis, M. Assessment of metal pollution and subsequent ecological risk in the coastal zone of the Olkhon Island, Lake Baikal, Russia. *Sci. Total Environ.* **2021**, *786*, 147441. [CrossRef] [PubMed]
15. Zhang, Y.; Su, J.; Jiang, W.; Huang, Z.; Xiang, Y.; Zeng, F. Study on the Heavy Metal Pollution Evaluation and Countermeasures of Middle Size and Small Cities in Typical Drainage Area-Taking Xiangtan Reach of Xiangjiang River as an Example. *Res. J. Chem. Environ.* **2012**, *16*, 172–179.
16. Jiang, F.; Ren, B.; Hursthouse, A.S.; Zhou, Y. Trace metal pollution in topsoil surrounding the Xiangtan manganese mine area (South-Central China): Source identification, spatial distribution and assessment of potential ecological risks. *Int. J. Environ. Res. Public Health* **2018**, *15*, 2412. [CrossRef] [PubMed]
17. Shi, X.; Ren, B.; Hursthouse, A. Source identification and groundwater health risk assessment of PTEs in the stormwater runoff in an abandoned mining area. *Environ. Geochem. Health* **2022**, *44*, 3555–3570. [CrossRef]
18. Xie, Q.; Ren, B. Pollution and risk assessment of heavy metals in rivers in the antimony capital of Xikuangshan. *Sci. Rep.* **2022**, *12*, 14393. [CrossRef] [PubMed]
19. Zhang, Y.; Ren, B.; Hursthouse, A.; Deng, R.; Hou, B. Leaching and releasing characteristics and regularities of Sb and As from antimony mining waste rocks. *Pol. J. Environ. Stud.* **2019**, *28*, 4017–4025. [CrossRef] [PubMed]
20. Zhou, Y.; Ren, B.; Hursthouse, A.S.; Zhou, S. Antimony Ore Tailings: Heavy Metals, Chemical Speciation, and Leaching Characteristics. *Pol. J. Environ. Stud.* **2019**, *28*, 485–495. [CrossRef]
21. Huang, T.; Chen, D.; Fu, Y.; Yeasmin, R.; Guo, C. Development and evolution of a euxinic wedge on the ferruginous outer shelf of the early Cambrian Yangtze sea. *Chem. Geol.* **2019**, *524*, 259–271. [CrossRef]
22. Ren, B.; Wang, C.; Ma, H.; Deng, R.; Zhang, P. Effect to rainfall on Sb release characteristics from smelting slag in rainy south China. *Fresenius Environ. Bull.* **2016**, *25*, 4908–4914.
23. Pan, L.C.; Hu, R.Z.; Wang, X.S.; Bi, X.W.; Zhu, J.J.; Li, C. Apatite trace element and halogen compositions as petrogenetic-metallogenic indicators: Examples from four granite plutons in the Sanjiang region, SW China. *Lithos* **2016**, *254*, 118–130. [CrossRef]
24. Kang, S.; Zhang, Q.; Zhang, Y.; Guo, W.; Ji, Z.; Shen, M.; Mayewski, P. Warming and thawing in the Mt. Everest region: A review of climate and environmental changes. *Earth-Sci. Rev.* **2022**, *225*, 103911. [CrossRef]
25. Tang, Z.E.; Deng, R.J.; Zhang, J.; Ren, B.Z.; Hursthouse, A. Regional distribution characteristics and ecological risk assessment of heavy metal pollution of different land use in an antimony mining area–Xikuangshan, China. *Hum. Ecol. Risk Assess. Int. J.* **2020**, *26*, 1779–1794. [CrossRef]
26. Xie, Q.; Ren, B.; Hursthouse, A.; Shi, X. Effects of mining activities on the distribution, controlling factors, and sources of metals in soils from the Xikuangshan South Mine, Hunan Province. *Integr. Environ. Assess. Manag.* **2022**, *18*, 748–756. [CrossRef]
27. Xie, Q.; Ren, B.; Shi, X.; Hursthouse, A. Factors on the distribution, migration, and leaching of potential toxic metals in the soil and risk assessment around the zinc smelter. *Ecol. Indic.* **2022**, *144*, 109502. [CrossRef]
28. Luo, X.; Ren, B.; Hursthouse, A.S.; Jiang, F.; Deng, R.J.; Wang, Z. Source identification and risk analysis of potentially toxic elements (PTEs) in rainwater runoff from a manganese mine (south central Hunan, China). *Water Supply* **2021**, *21*, 824–835. [CrossRef]
29. Church, S.E. Multi-element analysis of fifty-four geochemical reference samples using inductively coupled plasma-atomic emission spectrometry. *Geostand. Newsl.* **1981**, *5*, 133–160. [CrossRef]
30. Kang, J.; Li, C.; Dong, L.; Xiao, S. Early Diagenetic Dolomite as a Potential Archive of Paleo-redox Fluctuations in an Early Tonian Marine Basin? *Acta Geol. Sin. (Engl. Ed.)* **2022**, *96*, 607–620. [CrossRef]
31. Lin, Y.; Wang, S.; Yang, Z.; Zhao, Y.; Yang, Y. Characteristics of Hydrogen-rich Coals in Southern China: Implications from Organic Geochemistry and Carbon Isotopic Compositions. *Acta Geol. Sin. (Engl. Ed.)* **2022**, *96*, 309–320. [CrossRef]
32. Dai, D.; Bao, H.; Liu, S.; Yin, F. Oxygen Isotopic Compositions in a Plagioclase-Olivine Inclusion from Ningqiang Similar to Those in Al-rich Chondrules. *Acta Geol. Sin. (Engl. Ed.)* **2021**, *95*, 1583–1590. [CrossRef]
33. Singh, M.; Müller, G.; Singh, I.B. Heavy metals in freshly deposited stream sediments of rivers associated with urbanisation of the Ganga Plain, India. *Water Air Soil Pollut.* **2002**, *141*, 35–54. [CrossRef]

34. Saydam Eker, Ç. Distinct contamination indices for evaluating potentially toxic element levels in stream sediments: A case study of the Harşit Stream (NE Turkey). *Arab. J. Geosci.* **2020**, *13*, 1175. [CrossRef]
35. Ustaoğlu, F.; Islam, M.S. Potential toxic elements in sediment of some rivers at Giresun, Northeast Turkey: A preliminary assessment for ecotoxicological status and health risk. *Ecol. Indic.* **2020**, *113*, 106237. [CrossRef]
36. Kükrer, S.; Erginal, A.E.; Kılıç, Ş.; Bay, Ö.; Akarsu, T.; Öztura, E. Ecological risk assessment of surface sediments of Çardak Lagoon along a human disturbance gradient. *Environ. Monit. Assess.* **2020**, *192*, 359. [CrossRef]
37. Fural, Ş.; Kükrer, S.; Cürebal, İ. Geographical information systems based ecological risk analysis of metal accumulation in sediments of İkizcetepeler Dam Lake (Turkey). *Ecol. Indic.* **2020**, *119*, 106784. [CrossRef]
38. Park, M.; Chon, H.T.; Marton, L. Mobility and accumulation of selenium and its relationship with other heavy metals in the system rocks/soils–crops in areas covered by black shale in Korea. *J. Geochem. Explor.* **2010**, *107*, 161–168. [CrossRef]
39. Liu, Y.; Xiao, T.; Perkins, R.B.; Zhu, J.; Zhu, Z.; Xiong, Y.; Ning, Z. Geogenic cadmium pollution and potential health risks, with emphasis on black shale. *J. Geochem. Explor.* **2017**, *176*, 42–49. [CrossRef]
40. Zhao, Y.; Liu, Q.; Zhang, C.; Liao, J.; Lin, H.; Wang, Y. Coupled seepage-damage effect in fractured rock masses: Model development and a case study. *Int. J. Rock Mech. Min. Sci.* **2021**, *144*, 104822. [CrossRef]
41. Liu, J.; Zhao, Y.; Tan, T.; Zhang, L.; Zhu, S.; Xu, F. Evolution and modeling of mine water inflow and hazard characteristics in southern coalfields of China: A case of Meitanba mine. *Int. J. Min. Sci. Technol.* **2022**, *32*, 513–524. [CrossRef]
42. Xiao, Z.; Cao, Y.; Jiang, W.; Zhou, P.; Huang, Y.; Liu, J. Minerals and enrichment of W, Rb, and Cs in late Permian coal from Meitian mine, Meitian coalfield, Southern China by magmatic hydrothermal fluids. *Minerals* **2018**, *8*, 504. [CrossRef]
43. Turner, B.L.; Wells, A.; Andersen, K.M.; Condron, L.M. Consequences of the physical nature of the parent material for pedogenesis, nutrient availability, and succession in temperate rainforests. *Plant Soil* **2018**, *423*, 533–548. [CrossRef]
44. Zhang, Y.; Xiang, Y.B.; Chen, W.Y. Heavy metal content in the bark of camphora tree in Xiangtan and its environmental significance. *Appl. Ecol. Environ. Res.* **2019**, *17*, 9827–9835. [CrossRef]
45. Zhang, Y.; Zhao, C.; Chen, G.; Zhou, J.; Chen, Z.; Li, Z.; Chen, Y. Response of soil microbial communities to additions of straw biochar, iron oxide, and iron oxide–modified straw biochar in an arsenic-contaminated soil. *Environ. Sci. Pollut. Res.* **2020**, *27*, 23761–23768. [CrossRef]
46. Peng, J.S.; Guan, Y.H.; Lin, X.J.; Xu, X.J.; Xiao, L.; Wang, H.H.; Meng, S. Comparative understanding of metal hyperaccumulation in plants: A mini-review. *Environ. Geochem. Health* **2021**, *43*, 1599–1607. [CrossRef]
47. Yu, H.; Xiang, Y.; Zou, D. The effect of Eulaliopsis binata on the physi-chemical properties, microbial biomass, and enzymatic activities in Cd-Pb polluted soil. *Environ. Sci. Pollut. Res.* **2016**, *23*, 19212–19218. [CrossRef]
48. Zhang, Y.; Ren, B.; Hursthouse, A.S.; Deng, R.; Hou, B. An improved SWAT for predicting manganese pollution load at the soil-water interface in a manganese mine area. *Pol. J. Environ. Stud* **2018**, *27*, 2357–2365. [CrossRef]
49. Zhang, Y.; Ren, B.; Hursthouse, A.S.; Deng, R.; Hou, B. Study on the Migration Rules of Sb in Antimony Ore Soil Based on HYDRUS-1D. *Pol. J. Environ. Stud.* **2019**, *28*, 965–972. [CrossRef]
50. Cao, T.; Liu, G.; Liu, H.; Deng, M.; Han, Y.; Huang, Y.; Hursthouse, A.S. Nanoscale Pore Characteristics of the Upper Permian Mudrocks from a Transitional Environment in and around Eastern Sichuan Basin, China. *Acta Geol. Sin.-Engl. Ed.* **2019**, *93*, 1025–1046. [CrossRef]
51. Cao, T.; Liu, H.; Pan, A.; Fu, Y.; Deng, M.; Cao, Q.; Yu, Y. Pore evolution in siliceous shales and its influence on shale gas-bearing capacity in eastern Sichuan-western Hubei, China. *J. Pet. Sci. Eng.* **2022**, *208*, 109597. [CrossRef]
52. Xiao, Z.; Liu, J.; Tan, J.; Yang, R.; Hilton, J.; Zhou, P.; Cao, Y. Geologic characterization of a lower Cambrian marine shale: Implications for shale gas potential in northwestern Hunan, South China. *Interpretation* **2018**, *6*, T635–T647. [CrossRef]
53. Peng, B.; Rate, A.; Song, Z.; Yu, C.; Tang, X.; Xie, S.; Tan, C. Geochemistry of major and trace elements and Pb–Sr isotopes of a weathering profile developed on the Lower Cambrian black shales in central Hunan, China. *Appl. Geochem.* **2014**, *51*, 191–203. [CrossRef]
54. Peng, B.; Song, Z.; Tu, X.; Xiao, M.; Wu, F.; Lv, H. Release of heavy metals during weathering of the Lower Cambrian black shales in western Hunan, China. *Environ. Geol.* **2004**, *45*, 1137–1147. [CrossRef]
55. Zhao, W.; Song, Y.; Guan, D.; Ma, Q.; Guo, C.; Wen, Y.; Ji, J. Pollution status and bioavailability of heavy metals in soils of a typical black shale area. *J. Agro-Environ. Sci.* **2018**, *37*, 1332–1341.
56. Xu, Y.; Yang, R.; Zhang, J.; Gao, L.; Ni, X. Distribution and dispersion of heavy metals in the rock–soil–moss system of the black shale areas in the southeast of Guizhou Province, China. *Environ. Sci. Pollut. Res.* **2022**, *29*, 854–867. [CrossRef] [PubMed]
57. Wang, Y.; Wang, M.; Huang, B.; Li, S.; Lin, Y. Evaluation and Analysis of Poverty-Stricken Counties under the Framework of the UN Sustainable Development Goals: A Case Study of Hunan Province, China. *Remote Sens.* **2021**, *13*, 4778. [CrossRef]
58. Ponavic, M.; Pasava, J.; Vymazalova, A.; Kribek, B.; Deng, H.; Luo, T.; Zeng, M. Fractionation of toxic trace elements in soils around Mo-Ni black shale-hosted mines, Zunyi region, southern China: Environmental implications. *Bull. Geosci.* **2006**, *81*, 197–206. [CrossRef]
59. Turekian, K.K.; Wedepohl, K.H. Distribution of the elements in some major units of the earth's crust. *Geol. Soc. Am. Bull.* **1961**, *72*, 175–192. [CrossRef]
60. Nesbitt, H.W. Mobility and fractionation of rare earth elements during weathering of a granodiorite. *Nature* **1979**, *279*, 206–210. [CrossRef]
61. Huang, J.H.; Huang, F.; Evans, L.; Glasauer, S. Vanadium: Global (bio) geochemistry. *Chem. Geol.* **2015**, *417*, 68–89. [CrossRef]

62. Barbieri, M. The importance of enrichment factor (EF) and geoaccumulation index (Igeo) to evaluate the soil contamination. *J. Geol. Geophys* **2016**, *5*, 1–4. [CrossRef]
63. Salminen, R.; Tarvainen, T. The problem of defining geochemical baselines. A case study of selected elements and geological materials in Finland. *J. Geochem. Explor.* **1997**, *60*, 91–98. [CrossRef]
64. Singh, A.K.; Hasnain, S.I.; Banerjee, D.K. Grain size and geochemical partitioning of heavy metals in sediments of the Damodar River–a tributary of the lower Ganga, India. *Environ. Geol.* **1999**, *39*, 90–98. [CrossRef]
65. Muller, G. Index of geoaccumulation in sediments of the Rhine River. *Geojournal* **1969**, *2*, 108–118.

Disclaimer/Publisher's Note: The statements, opinions and data contained in all publications are solely those of the individual author(s) and contributor(s) and not of MDPI and/or the editor(s). MDPI and/or the editor(s) disclaim responsibility for any injury to people or property resulting from any ideas, methods, instructions or products referred to in the content.